

Four-Dimensional Realistic Modeling of Pancreatic Organogenesis

Yaki Setty*[†] Irun R. Cohen[‡] Yuval Dor[§] and David Harel[†]

*Computational Biology Group, Microsoft Research Limited, Cambridge CB3 0FB, UK,[†]Department of Computer Science and Applied Mathematics, Weizmann Institute of Science, Rehovot 76100, Israel,[‡]Department of Immunology, Weizmann Institute of Science, Rehovot 76100, Israel, and [§]Department of Cellular Biochemistry and Human Genetics, Hadassah Medical school, The Hebrew University, Jerusalem, Israel.

Submitted to Proceedings of the National Academy of Sciences of the United States of America

Classification:

Major: Biological Sciences, Minor: Developmental Biology.
Major: Physical Sciences, Minor: Computer Sciences

Correspondence author:

Prof. David Harel
Dept. of Computer Science and Applied Mathematics
The Weizmann Institute of Science Rehovot 76100, ISRAEL
Tel: +972-8-934-4050 (secretary: +972-8-934-3545)
Fax: +972-8-934-6023
email: david.harel@weizmann.ac.il
URL: <http://www.wisdom.weizmann.ac.il/~dharel>

Manuscript information:

9 text pages (including references and figure legend).
11 figures.

Reserved for Publication Footnotes

Organogenesis, the process by which organs develop from individual precursor stem cells, requires that the precursor cells proliferate, differentiate and aggregate to form a functioning structure. This process progresses through changes in 4 dimensions: time and three dimensions of space — 4D. Experimental analysis of organogenesis, by its nature, cuts the 4D developmental process into static, 2D histological images or into molecular or cellular markers and interactions with little or no spatial dimensionality and minimal dynamics. Understanding organogenesis requires integration of the piecemeal experimental data into a running, realistic and interactive 4D simulation that allows experimentation and hypothesis testing *in silico*. Here we describe a fully executable, interactive, visual model for 4D simulation of organogenic development using the mouse pancreas as a representative case. Execution of the model provided a dynamic description of pancreas development, culminating in a structure that remarkably recapitulated morphologic features seen in the embryonic pancreas. *In silico* mutations in key signaling molecules resulted in altered patterning of the developing pancreas, that were in general agreement with *in vivo* data. The modeling approach described here thus typifies a useful platform for studying organogenesis as a phenomenon in 4 dimensions. This paper is supplemented by a website (www.wisdom.weizmann.ac.il/~yaki/organogenesis), which contains recordings of the simulation, related data and appendices, as detailed in various places in the text.

computational modeling | pancreas | organogenesis | 4D modeling

Organogenesis and morphogenesis have been of interest to many scientists in different fields for a long time. Understanding organogenesis not only explains how biological systems are formed, but can also offer insight into their evolution (e.g., the shape of a leaf is in part an adjustment to varying habitats). In this paper we present a generic approach to the realistic 4D modeling of organogenesis based on experimental data. Furthermore, we describe how we applied this approach to modeling pancreatic organogenesis.

4D modeling

Organogenesis, the development of a functioning, anatomically specialized organ from a relatively small number of relatively undifferentiated precursor cells, is critically influenced by factors involving multiple scales, dynamics and 3D anatomic relationships. The importance of scales is evident in the scale-crossing chain of genetic and chemical reactions leading to cellular behavior and anatomic structuring that, in turn, feeds back down the scales to influence gene expression; indeed, the emergence of many important properties of living systems needs to take account of interactions that take place across different scales [1]. The importance of dynamics is evident in the time-dependency of developmental processes at every scale. And the importance of 3D anatomy is evident in the specific structure of the developing organ and its dependence on interactions with adjacent cells and molecular inducers.

Experimental data, because of the analytical nature of science, rarely, if ever, provide a smooth transition across scales; they are usually limited to snapshots of processes in place of dynamics, and furnish only very crude, if any 3D information. Since scale, dynamics and 3D anatomy are of the essence in organogenesis, an adequate understanding of the process would be greatly enhanced by tools that would be able to integrate the piecemeal, static and isolated experimental data into precisely flowing and trans-scaler 4D models. Moreover, the value of such modeling would be greatly enhanced if it would allow experimentation and hypothesis testing *in silico* as a guide to biological experimentation and if the modeling interface would provide visual representations intuitively comprehensible to experimentalists. This paper reports a first step in developing a realistic 4D approach to organogenesis.

The modeling approach

In the current study, we focused on the development of the pancreas, a compound organ with a unique structure, essential for the exocrine digestion of foodstuffs and for the hormonal regulation of metabolism. We integrated the known mechanisms and processes, including histological images, using Reactive Animation [2], a previously developed technique that links a reactive executable-model with an animated front-end to form a visualized, interactive and dynamic model. Previously, Reactive Animation was employed to model T cell proliferation in the thymus gland and to model development of the lymph node, using a reactive model that was linked to a 2D interactive front-end [2, 3, 4]. For the current work, we extended Reactive Animation and designed a generic platform that enables interaction between reactive engines, 3D animation and real-time analysis [5].

We formalized pancreatic organogenesis as an autonomous agent system [6], by specifying Statecharts [7] for organogenesis of the pancreas (using the Rhapsody tool [8]). We defined a cell, the basic building block of an organ, as an entity that senses environmental signals and responds to them. In addition, we modeled the environment that surrounds the pancreas and supplies important inducing signals. To better visualize and manipulate the simulation, we linked the model to a 3D animated front-end (in 3DGAMESTUDIO [9]) and to a mathematical GUI (in MATLAB [10]). At run-time, the front-end visualizes the simulation continuously and provides the means to interact with it. Separately, the mathematical GUI provides statistics and graphs of the simulation.

We present here a model that covers the primary stages of pancreatic organogenesis in the mouse. Although it is a partial introduction to a complex subject, the model has already furnished new insights. We tested the model by comparing the results against related experimental data and theoretical work. Generally, the simulation captured pancreatic organogenesis and provided a dynamic description of the system. In particular, *in silico* analysis of the morphogenesis emerging from the simulation revealed a close visual resemblance to histological images of the pancreas. Although we did not have anything like this in mind when we started out, and although the model was not explicitly programmed to do so, the simulation gave rise to an emergent property that corresponds well with the primary transition clusters appearing early in the developing organ *in vivo* [11, 12, 13]. Furthermore, we compared the

simulation with *in vivo* ablation experiments of tissues in the surrounding environment by reproducing experimental results *in silico*. The results agreed with the biology by reproducing similar results and provided a dynamic analysis of the experiments. In addition, results of certain mechanisms in the model produced patterns similar to related theoretical work.

Pancreatic organogenesis

In mice, pancreatic organogenesis is initiated at the eighth embryonic day, and is roughly divided into two transitions, primary and secondary [14]. During the *primary transition*, cells at the appropriate regions of the flat gut are specified as pancreatic and form a bud; during the *secondary transition*, the bud evolves to become a lobulated structure (Figure 1, top) [11, 15, 16]. At the same period, a cell-cell interaction mediated by the Delta-Notch mechanism directs cells towards an exocrine or endocrine fate by activating expression of specific markers (e.g., the endocrine marker *ngn3*) [11, 17]. The organogenesis process terminates when endocrine cells aggregate to form many sphere-like endocrine tissues, the *islets of Langerhans*, embedded within the exocrine pancreas. The pancreas develops simultaneously from a ventral site and a dorsal site; during organogenesis the ventral pancreas associates with the significantly larger dorsal pancreas [18].¹

Organogenesis depends on simultaneous interactions across different scales: molecular and morphogenetic mechanisms act in concert to form an organ. The molecular mechanisms involve processes that regulate the differentiation and development of individual cells, whereas the morphogenetic mechanisms gather the cells together to form a cauliflower-shaped organ. These processes do not occur independently, but decisively affect each other. For example, the spatial location of a cell governs its molecular decisions, and, vice versa, the state of differentiation of a cell influences its spatial location [19, 20, 21, 22]. Furthermore, studies have shown that mice lacking a normal extracellular matrix (ECM) around the developing pancreatic tissue fail to develop the organ. Thus, the ECM plays a crucial role in pancreatic organogenesis by generating signals that trigger intra-cellular processes, such as gene expression [23, 24, 25]. These intra-cellular processes govern cell function and cell migration.

An example of such a signaling process is pancreatic specification, which directs endodermal cells towards a pancreatic fate. Specification largely depends on two external signals from the notochord, *activin β* and *FGF2*. These signals inhibit expression of proteins that repress the expression of the pancreatic marker, *Pdx1* [26, 27, 28, 29]. Hence, an endodermal cell will not be specified as pancreatic unless it receives both signals from the notochord.

Section Results

The molecular model generates histology

We tested the simulation by comparing the emerging structure against histological sections of the pancreas at different stages that correspond to the illustration in Figure 1; see Figure 4. We also compared the results to 2D illustration of pancreatic organogenesis (Figure 5; left part adopted from [13]). Furthermore, we analyzed the simulation against a 2D histological image of pancreatic morphogenesis at the tenth embryonic day (Figure 6 top-left). The image provides a fluorescent cross-section of a pancreatic bud, in which *Pdx1*-positive cells are stained in green, whereas, *Pdx1*-negative cells are labeled in red. We compared the image against two different perspectives (Figure 6 bottom) and a cross-section image (Figure 6 right-top) of the simulation, approximately at the same period. The simulation corresponds well with the histology, indicating that the 3D structure emerging from the simulation seems to capture pancreatic morphogenesis in the mouse. We also found visual similarity between the emerging structure and 3D histology of the pancreas (adopted from [30, 31]). The relevant clips are attached to the supplementary material and are available at www.wisdom.weizmann.ac.il/~yaki/organogenesis.

The emerging structure is specific

To test whether the resemblance of the emerging *in silico* structure to the *in vivo* morphology of the developing pancreas depended on the specific molecular connection ‘rules’ integrated into our model, we randomized the expression of genes in the nucleus in a way that keeps the same state characteristics as the original statechart. Each state in the randomized statechart has the same number of incoming and outgoing transitions as the corresponding state had in the original statechart (see e.g., Figure 1 in supplemental Appendix C). Based on this setup, the emerging structure of the pancreas failed to develop the initial bud (see Figure 2 in supplemental Appendix C). This control experiment indicates that the 3D structure emerging from the model is a consequence of specific molecular information specified in the model, rather than a global tendency of the model to develop into a cauliflower-shaped structure.

Emergence of primary transition clusters

During the morphogenetic analysis, we noticed that the simulation, although never explicitly programmed to do so, exhibited clusters of pancreatic cells not expressing the key pancreatic gene *Pdx1*, but embedded deep in the epithelium of the pancreas. (Figure 6, bottom). These clusters are reminiscent of a group of cells observed *in vivo* in the early pancreas, termed *primary transition cells*. *In vivo* primary transition cells do not express *Pdx1*, but

¹In the current work, we focused on the dorsal pancreatic development and left out the similar process at the ventral tissue. However, the model is modular enough to be extended to cover the ventral development as well.

express hormones (often both insulin and glucagon). The *in silico* clusters aggregated at the top of the bud similarly to clusters of primary transition cells *in vivo*. Preliminary analysis revealed that early endocrine cells, like those in the simulation, do not express the pancreatic marker Pdx1 [11]. Further study suggests that primary transition cells do not appear in the mature organ and probably migrate, or undergo apoptosis [12, 32]. For the sake of simplicity, we assumed that such cells die later in development and therefore do not appear in the mature organ.

Analyzing the model revealed that the Pdx1-negative pancreatic cells achieved a maximum at approximately day 10, when an average of $\sim 4\%$ of the cells were Pdx1-negative (Figure 7, left). We then calculated the frequency of primary transition cells *in vivo* by analyzing images of the pancreatic buds stained for Pdx1 and glucagon and taken using a confocal microscope (Figure 8). Interestingly, the frequency of primary transition cells in these embryos ($\sim 6\%$) was similar to the observed frequency in the model.

The model suggests that the origin of this population is from cells that never expressed Pdx1, but were rather "trapped" in the budding epithelium. *In vivo* lineage tracing experiments can provide a definitive test of this prediction. The model also shows that these clusters are formed by cells with a common ancestor and thus are a consequence of proliferation rather than aggregation. We are currently looking for ways to examine this prediction experimentally.

It is important to acknowledge that the modeling data do not prove that Pdx1-negative cell clusters are the *in silico* manifestation of primary transition cells. However, there are intriguing similarities between the two populations that beg this conclusion: *in vivo* and *in silico* cell populations appear at similar times during embryonic development and later disappear; both populations are Pdx1-negative; and the location of these cells, their overall frequency and their cluster size are also similar between *in vivo* and *in silico* populations.

The model fits theory

The aforementioned Delta-Notch (DN) mechanism widely directs differentiation in multicellular organisms [17, 11]. As mentioned above, in pancreatic organogenesis, DN is involved in directing pancreatic cells towards an endocrine fate [17]. This mechanism is the focus of much theoretical work and has been modeled using various approaches, such as ODE, hybrid automata, Petri nets and more (see, e.g., [33, 34, 35]).

To compare our model with other work, we disabled certain processes in the simulation, such as proliferation and migration. In this experiment, cells on the initial flat sheet can interact with their neighboring cells but cannot proliferate or migrate. When equilibrium is achieved (i.e., more interactions between cells do not end with further differentiation), the simulation displays small clusters of endocrine cells scattered in a sheet of pancreatic progenitor cells (Figure 7, right). Results of other theoretical work suggested a similar pattern, in which cells of a certain type scattered among cells of a different type. The clusters that appear in our simulation may be related to the Langerhans islets, sphere-like aggregations of endocrine cells that appear in the mature pancreas. On average, the simulation achieved equilibrium after one embryonic day when $\sim 15\%$ of the cells ended up as endocrine cells (Figure 7, right).

The model anticipates experimental findings

We further tested the model by reproducing ablation experiments, in which the organism was engineered to lack certain tissues. To simulate such experiments, we disabled the function of relevant objects in the running simulation. Generally, our results captured the essence of similar *in vivo* experiments and provided a dynamic molecular and morphogenetic analysis (Figure 9). When we disabled the notochord, the Notochord related factors, in particular FGF2 and activin β were not secreted to the ECM (i.e., the concentrations of these factors in the grid were below their thresholds). As these factors regulate pancreatic specification, none of the cells were specified as pancreatic (i.e., the molecular mechanisms of specification were blocked). Interestingly, other morphogenetic processes were partly damaged; cells gathered to form the initial bud, but failed to develop the mature lobulated organ (Figure 9, middle). The results are consistent with similar *in vivo* experiments, in which ablation of the notochord showed a bud that was not specified as pancreatic [36, 26, 27, 16]. The histological 2D section (Figure 9 middle right) shows the pancreatic bud that formed in a mouse lacking the notochord (H and E staining; adopted from [37]). As in the simulation, a branched bud was formed but was not specified as pancreatic (i.e., cells did not express the pancreatic marker Pdx1).

In a similar experiment, the aorta was disabled and thus the concentrations of the BMP4 and FGF10 factors, which promote budding of pancreatic cells, were below their thresholds [38, 24]. The results in this case showed that cells were specified normally as pancreatic, but failed to form the initial pancreatic bud (Figure 9, bottom). Furthermore, the cell population was reduced in size indicating that proliferation was partly damaged. The results concur with similar *in vivo* experiments, which showed pancreatic cells that did not form a pancreatic bud. The 2D histological section image (Figure 9, bottom right; adopted from [38]) displays the endodermal tissue, which was specified as pancreatic but failed to form a bud (i.e., it expressed the pancreatic marker Pdx1 but did not form a structure).

The model discloses morphogenetic behavior

As mentioned above, pancreatic organogenesis is largely regulated by factors in the ECM that promote signaling in cells. Two factors, BMP4 and FGF10, promote pancreatic morphogenesis at the primary stages of the organogenesis [39, 40, 41]. BMP4 is the first to be expressed and promotes budding formation, whereas FGF10 is expressed later and promotes (among other things) patterning of the pancreatic bud [42]. The tissues surrounding the pancreas regulate the concentrations of the mesenchymal factors [24, 43, 13]. In our model, we defined areas in the extracellular space that contain different concentrations of these two factors. At run time, concentrations are regulated by various objects, in particular by the Aorta object which also govern the blood vessels.

Theoretically, we may define infinitely many possible distributions of the factors in space, each described by an arrangement and a regulation effect (i.e., the way it promotes the factors in its vicinity) of blood vessels. Accordingly, the pancreatic structure, which emerged earlier, is described by a specific blood vessel layout and effect. In this section, we go beyond the simple ablation experiments discussed above and use the model to study pancreatic morphogenesis more generally by mutating the factors in the environment to extreme cases.

To study the role of the FGF10 and BMP4 factors on pancreatic morphogenesis, we mutated the blood vessels in the space. At this stage, we preserved the layout of the arteries and mutated only their effect (i.e., the way they regulate BMP4 and FGF10 concentrations). We programmed the arteries to promote three different levels of expression for each factor — low, normal and high. Figure 10 displays snapshots of the simulation at equilibrium under the nine possibilities. The results show that when the expression level of FGF10 was increased the morphogenesis tended towards a more branched structure. Likewise, when the expression level of BMP4 was increased the morphogenesis tended towards a more lobed structure. The extreme expression levels of the factors revealed an intensified impact of the factors when one was increased and the other was decreased. Decreasing FGF10 expression and increasing BMP4 expression led to a single lobe at the top of the pancreatic bud. Likewise, decreasing FGF10 expression and increasing BMP4 expression led to rather long finger-like structures. Interestingly, decreasing the expression of both factors led to a chaotic behavior of pancreatic cells and a loss of structure; whereas increasing both factors led to a hyperplastic morphogenesis and an enlarged Pdx1-negative population.

In more advanced experiments, we mutated not only the effect of the blood vessels but also its positioning. Accordingly, we changed the layout of the blood vessels to promote different distributions of factors (i.e., FGF10 and BMP4) in the environment. The model revealed shapes that are different in nature from the genuine pancreatic structure. Initially, we defined condensed arteries, which promote a weak uniform expression of FGF10 and a strong concentrated expression of BMP4. Under these environmental conditions the emerging structure was a massive lobed pancreas, somewhat similar to the shape of the liver (Figure 11, left). Further, we defined a branched blood-vessel layout, which promoted a scattered expression of FGF10 and a uniform expression of BMP4. The emerging structure was highly branched, somewhat similar to the shape of the lungs (Figure 11, right). These results appear to describe how two independent and concurrent mechanisms generate the lobulated form by promoting behavior in individual cells. Interestingly, the aforementioned foregut organs, namely the liver and the lungs, are exposed to similar factors during their organogenesis [40, 44, 45, 46, 47, 48]. These results suggest that blood vessels could play a role in branching morphogenesis of the embryonic pancreas, a prediction yet to be tested by *in vivo* experiments.

Section Discussion

The modeling of early pancreatic organogenesis described here suggests that it is useful to integrate experimental data into a running 4D simulation. 4D modeling can indeed provide a seamless and integrated view of a complex process that we usually analyze through piecemeal experimentation. The integration is illuminating:

Multi-scale: 4D makes visually comprehensible the many scales of interaction that proceed concurrently — genetic, molecular, intra-cellular, inter-cellular, environmental, inter-organ, and so forth.

Cross-scale: We see how organ structure and environment can determine molecular interactions; and vice versa, how molecular interactions can determine structure and environment.

Emergence: 4D discloses the emergence of new properties as the process unfolds across scales — molecular interactions lead to 3D organ structure.

Dynamics: Change with time, the essence of development, is visually perceptible.

It would appear that the 4D modeling is empowering as well as illuminating. Here we demonstrate that we can carry out experiments *in silico*, which cannot replace ‘wet-lab’ experimentation but can help direct the experimenter towards the more decisive experiment, saving time, resources and animal manipulations.

Formulating and testing hypotheses, as we show here, are also feasible in 4D simulation. No less important, the very attempt to collect the data needed for a 4D model highlights missing data and directs our attention to key experimental questions that experimenters did not consider or did not believe worthwhile to ask; Thus, modeling extends awareness.

During the last few years, increasing interdisciplinary work combines experimental results with theoretical models to explain the morphogenesis of different systems (see e.g., [49, 50, 51, 52]). Most of this work, unlike the present modeling, ignores multiple concurrent activities and focuses on a single mechanism in the system. The approach we employed here, based on Reactive Animation, integrates the piecemeal, static experimental data into a reactive model that is linked to a 3D animated front-end for visualization and to a mathematical GUI for analysis. As data accumulate, in particular data related to dynamic and morphogenetic aspects, the model may be further tested, calibrated and extended.

In the case of pancreatic organogenesis, we started with a version of a ‘divide and conquer’ concept, which is guided by decomposing a system into independent modules and reassembling them at run-time. Accordingly, we defined two main modules, one specified the structural development based on sweeps-to-branched-skeleton algorithms [53], and the other formalized the molecular interactions in an individual cell.

Although we found that this approach gave rise to some interesting ideas, it could not capture faithfully the process of organogenesis (see [54]). As we continued to study the process, we advanced to the autonomous agent concept [6], which does not carry any artificial objects and thus seems more suitable for modeling biology. Accordingly, we

defined a cell as an autonomous entity that senses the factors in its near environment and modeled the environment that surrounds the pancreas, which supplies important inducing signals. Pancreatic organogenesis, as it emerged from the model, qualitatively reproduced similar structure as in relevant histology; it starts from a flat sheet of cells and evolves to a lobed structure through budding and branching processes. Furthermore, the model anticipates *in vivo* observations, fits theoretical results of related work on the actual processes, gives rise to intriguing novel ideas about pancreatic morphogenesis and points to the possibility of analogous processes in morphogenesis in the liver and lungs.

We envision the future development of this work in two separate directions. First, we are in the process of extending coverage of the model to capture, among other things, the formation of the endocrine islets of Langerhans buried within the exocrine pancreas. We believe that in the long run the pancreatic model may serve for carrying out *in silico* experiments that may lead to a better understanding of the pancreas and of pancreas-related diseases, such as diabetes. Secondly, the model may serve as a starting point for modeling organogenesis in other systems in biology, and it may help in the efforts to design an *in silico* organ or organism (see e.g., [55, 56, 57, 1, 58, 59]). To this end, we are in the process of examining the possibility of using the same approach to model the development of the *C. elegans* nematode, which is extensively used as a model organism in molecular and developmental biology.

Section Methods

Modeling technique

To specify behavior of objects in the model, we use the language of Statecharts [7, 60], as it is implemented in the Rhapsody tool [8]. Statecharts define behavior using a hierarchy of states with transitions, events, and conditions. The language can be compiled into executable code using Rhapsody.

We linked the model to a 3D animated front-end (in 3DGameStudio [9]), which visualizes the simulation and provides the means to interact with it. At run time, processes in the simulation are reflected in the front-end in different ways, e.g., by color and position changes. Furthermore, the model is linked to a mathematical analysis GUI (using MATLAB) that displays various graphs and statistics of the simulation. A prerecorded run of the simulation is available at www.wisdom.weizmann.ac.il/~yaki/runs.

Using ideas from the Turing instability hypothesis [61, 62], we adjusted the autonomous agent concept [6, 63], widely used in artificial intelligence, to morphogenesis. Using statecharts, we modeled the extracellular space and specified the eukaryotic cell as an autonomous agent, i.e., an independent object that acts to change the environment and influences what it senses at a later time. This concept, which considers a cell as the basic building block, is highly suitable for modeling organogenesis, as it evolves by a cell population whose individual elements act in concert. The supplementary material for this manuscript contains two documents that provide details of the model. Appendix A details the biological elements that were included in the model, and Appendix B describes the statechart model of the cell in greater detail.

Modeling an autonomous cell

The behavior of the eukaryotic cell, which is the basic element of the model, is specified using three distinct objects, namely the **Nucleus**, **Membrane**, and **Cell**. The **Cell** includes the specification of the different stages in the life-cycle of the eukaryotic cell, and consists of the two other objects. The **Nucleus** object specifies gene expression in the **Cell** in a discrete fashion, whereas the **Membrane** object specifies the **Cell**'s response to external stimulations.

This setup is illustrated in Figure 2, which shows the three objects and (parts of) their statecharts. The statechart of the **Cell** object contains two concurrent components, specifying the **Proliferation** and **Differentiation** processes. The **Proliferation** component defines a state for each stage of the cell cycle, whereas the **Differentiation** component specifies a state for each developmental stage. The **Nucleus** and the **Membrane** objects are located inside the **Cell** to indicate the (strong) composition relation between the three objects, i.e., that the **Nucleus** and the **Membrane** cannot exist without the **Cell** containing them. The statechart for the **Nucleus** specifies each gene as an independent component that can be either in an **Expressed** state or an **Unexpressed** state (in Figure 2, these states are denoted by **Exp.** and **Unexp.**, respectively). Figure 2 shows the components of *Sonic hedgehog* (**Shh**), *Patched* (**Ptc**), and *Pdx1*, three of the genes involved in pancreatic organogenesis. Similarly, the statechart for the **Membrane** specifies the cell's reactions to possible external stimulations. Two sub-components within the **Membrane** statechart in Figure 2 specify the behavior of two receptors in the **Membrane**, *activin receptor* **AcrR**, and *fibroblast growth factor receptor* **FGFR**. The receptors can either be in a **Bound** state or an **Unbound** state. The third component in the **Membrane** statechart depicts the **Motion Unit** that continuously scans over the 6 possible directions to find the optimal move. The states themselves contain behavioral instructions for the cell. For example, in the **Membrane** the state **Bound** of a receptor defines the specific genes it activates. Similarly, in the **Nucleus** the **Expressed** state contains instructions for genes to activate the expression of other genes. Which genes and which receptors affect which genes were specified according to data collected from the published literature on pancreas development. For example, inactivation of the **SHH** gene induces the expression of **Ptc**.

At the front-end, the **Cell** is visualized as a sphere that changes properties to indicate molecular stages. For example, a red sphere denotes a **Cell** in an **Endoderm** state, whereas a green sphere denotes a **Cell** in a **Pancreas progenitor** state (Figure 2, top-left). This formalization defines the **Cell** as a 3D animated autonomous entity that senses the environment and behaves accordingly.

Modeling the extracellular space

To model the extracellular space surrounding the pancreas, we defined an object representing the **Extracellular Matrix** (ECM), handling a 3D grid that overlays the pancreatic tissue. Accordingly, the space surrounding the organ is divided into 3D grid-cubes with a fixed volume. The three tissues in the extracellular space – **Notochord**, **Aorta**, and **Mesenchyme** – are defined as objects, and their behavior is specified based on what is recorded in the literature (see, e.g., [11, 19]). These tissues are known to promote early stages of pancreatic development by secreting factors in the ECM. In the model, concentrations of relevant factors are stored in the ECM grid-cubes and can be updated by the tissue objects (i.e., the **Notochord**, **Aorta** and **Mesenchyme**). For example, the notochord secretes several factors in the extracellular space, thus, in our model, the **Notochord** object regulates concentrations of relevant factors in the ECM grid next to its specified location.

Based on the literature (e.g., Figure 3, top) we designed an animated front-end (Figure 3, middle) that visualizes the extracellular space in the model. Specifically, in the front-end, the **Mesenchyme** is represented by a tissue-like space that changes its color when the **Aorta** is present. A long tube, representing the endodermal **Gut**, lies at the center of the ECM. The **Notochord**, when it exists, is represented by a transparent green tube that lies above the **Gut**. The behavior of the **Gut** is outside the scope of the model and serves for visualization purposes solely.

The interaction scheme of the model is illustrated in Figure 3, bottom, where an interaction is feasible if a line connects two objects. For example, the **Notochord** may interact with the ECM but cannot interact directly with the **Mesenchyme**. To be faithful to the biology, we prevented direct interaction between tissues and **Cells**. Nevertheless, cells indirectly interact with tissues when they sense concentrations of factors in the ECM that were previously produced by a tissue.

The simulation at run-time

Consider the **Cell** and its partial statecharts in Figure 2 and the animated front-end in Figure 3middle. When the model is executed, instances of the **Cell** are created and appear in the front-end as a sheet of red spheres on the proper location at the flat endodermal **Gut**. Once a **Cell** instance is created, one state in each concurrent component of its statechart is set to be an active state. At this point, the **Cells** are uniform and their active states are set to the initial states (designated by a stubbed arrow). In parallel, the environment is initiated and defines the initial concentrations of factors in the ECM (e.g., by secreting **activin β** and **FGF2** from the notochord). As the simulation advances, cells respond to various events (e.g., the concentration of factors in their vicinity) by changing their active states accordingly. Hence, the sheet loses uniformity at a very early stage of the simulation.

To illustrate the simulation in progress, we describe some of the processes a typical **Cell** undergoes during its life cycle. As a representative example, consider the aforementioned specification process that promotes expression of pancreatic genes in individual cells. As the simulation advances, endodermal **Cells** sense the concentrations of two factors, **activin β** and **FGF2**, both regulated by the **Notochord**. When a **Cell** senses that the concentration of **activin β** goes above a certain threshold, its **Membrane** generates an event that moves the active state of the **ActR** component to **Bound**. Similarly, the **Membrane** generates an event that moves the active state of the **FGFR** component to state **Bound** when the concentration of **FGF2** is above a certain threshold. When the active states of **FGFR** and **ActR** are set to **Bound**, an event is generated and the active state of the **Shh** gene in the **Nucleus** moves to state **Unexpressed**. Consequently, the active state of **Ptc** is set to state **Expressed** and initiates a cascade of events that eventually move the active state of **Pdx1** to **Expressed** (i.e., this instance of **Cell** expresses the pancreatic marker). In turn, an event is generated and the active state in the **Differentiation** component of the **Cell** moves from state **Endoderm** to state **Pancreas progenitor**. Accordingly, the corresponding animated sphere changes its color from red to green, indicating that pancreatic specification has been accomplished.

Concurrently, the active state of the **Proliferation** component moves through the different stages of the cell cycle to carry out cell division. When the active state moves to the state **M**, the **Cell** duplicates itself by creating an identical **Cell** instance. Accordingly, at the proper location in the front-end, a new identical sphere, corresponding to the new **Cell** instance, is created. However, if at any stage of the process the cell cannot proceed with the **Proliferation** (e.g., the appearance of an environmental signal), an event is generated and the active state in the component moves to state **G0** (i.e., the cell division is blocked). Further, proliferation is regulated by various mesenchymal factors, hence, the **Membrane** may generate events that accelerate the process.

During organogenesis, mesenchymal factors, such as **BMP4** and **FGF10**, promote the aggregation of cells. Therefore, we specified a **Motion Unit** in the **Membrane** that senses relevant factors. When the **Membrane** senses a gradient of relevant factors towards a certain axis, it initiates a cascade of events that update, if possible, the cell's position accordingly. For example, if the **Cell** senses a concentration gradient of a relevant factor towards its left on the **X** axis, the **Membrane** generates events that move the active state of the **Motion Unit** to state **X** and then to state **Left**. At the end of the process, the cell is located in a new position and the active state returns to state **Sense**. If at any stage the **Cell** cannot move, the **Membrane** generates an event and the active state in the **Motion Unit** is back to state **Sense**.

In the simulation, we assume that **Cells** die, i.e., undergo apoptosis, in the rare cases where cells encounter unpredicted situations (e.g., cells that, at an advanced stage of the simulation, express the wrong genes). A **Cell** that encounters such a situation generates an event that sets the active state of its entire statechart to **Dead**.

At a later stage of the organogenesis, the Cell initiates the cell-cell Delta-Notch (DN) mechanism, which, among other things, promotes the expression of the endocrine marker *ngn3*. Once initiated, the DN component of the Membrane continuously searches for cells in its close vicinity. When a neighboring cell is found, the two Cells interact and the Delta protein level in the Nucleus increases. When the level of Delta protein crosses a predefined threshold the active state of the *ngn3* gene moves to Expressed state. In turn, an event is generated and the active state at the Differentiation component in the Cell moves to Endocrine. Consequently, the corresponding sphere changes its color to purple. The principles behind DN specification are similar to the other processes described earlier. Therefore, for simplicity, we did not show DN in Figure 2. The complete related data are available at www.wisdom.weizmann.ac.il/~yaki/DN.

As a population, the Cells act in concert to drive the simulation by promoting various decisions in individual cells. Finally, the simulation achieves equilibrium when the cells are differentiated and are located at the available grid-voxel where they can no longer proliferate. Prerecorded clips of different stages of the simulation are available as supplementary material and at www.wisdom.weizmann.ac.il/~yaki/organogenesis

ACKNOWLEDGMENTS. This research was supported in part by The John von Neumann Minerva Center for the Development of Reactive Systems, and by a grant from the Kahn Fund for Systems Biology, both at the Weizmann Institute of Science. Part of David Harel's work carried out during a visit to the School of Informatics at the University of Edinburgh, which was supported by a grant from the EPSRC.

Special thanks go to Avi Mayo for his help in setting up the platform for modeling the extra-cellular environment. We also thank Judith Magenheim for providing histological images of the pancreas.

Permissions: Data in Figures 1, 4 and 9, reprinted by permission from Macmillan Publishers Ltd: *Nat Rev Genet* [19], copyright (2002). Data in Figures 3 and 5, reprinted from [13], Copyright (2002), with permission from Elsevier. Data in Figure 9 [37, 38] reproduced with permission of the Company of Biologists. Data in Figures 6 and 8 [11] reprinted with permission of Wiley-Liss, Inc., a subsidiary of John Wiley & Sons, Inc.

1. Cohen I. R., Harel D. (2007) Explaining a Complex Living System: Dynamics, Multi-scaling and Emergence *J R Soc Interface* 4:175–182.
2. Efroni S., Harel D., Cohen I. R. (2005) Reactive Animation: Realistic Modeling of Complex Dynamic Systems *IEEE Computer* 38:38–47.
3. Efroni S., Harel D., Cohen I. R. (2007) Emergent Dynamics of Thymocyte Development and Lineage Determination *PLoS Comput Biol* 3:e13.
4. Swerdlin N., Cohen I.R., Harel D. (2008) The Lymph Node B Cell Immune Response: Dynamic Analysis in-silico, in *Proceedings of the IEEE, special issue on Computational System Biology*, Vol 96, pp. 1421–1443.
5. Harel D., Setty Y. (2008) Generic Reactive Animation: Realistic Modeling of Complex Natural Systems, in *Formal Methods in Systems Biology*, pp. 1–16.
6. Brooks R. A. (1990) Elephants Don't Play Chess *Robotics and Autonomous Systems* 6:3–15.
7. Harel D. (1987) Statecharts: A Visual Formalism for Complex Systems *Sci. Comput. Programming* 8:231–274.
8. Telelogic, www.telelogic.com.
9. 3D Game Studio, www.3dgamestudio.com.
10. The MathWorks, www.mathworks.com.
11. Jensen J. (2004) Gene regulatory factors in pancreatic development *Dev Dyn* 229:176–200.
12. Herrera P. L. (2000) Adult insulin- and glucagon-producing cells differentiate from two independent cell lineages *Development* 127:2317–2322.
13. Kim S. K., MacDonald R. J. (2002) Signaling and transcriptional control of pancreatic organogenesis *Curr Opin Genet Dev* 12:540–547.
14. Pictet R. L., Clark W. R., Williams R. H., Rutter W. J. (1972) An ultrastructural analysis of the developing embryonic pancreas *Dev Biol* 29:436–467.
15. Slack J. M. (1995) Developmental biology of the pancreas *Development* 121:1569–1580.
16. Kim S. K., Melton D. A. (1998) Pancreas development is promoted by cyclopamine, a hedgehog signaling inhibitor *Proc Natl Acad Sci U S A* 95:13036–13041.
17. Chu K., Nemoz-Gaillard E., Tsai M. J. (2001) BETA2 and pancreatic islet development *Recent Prog Horm Res* 56:23–46.
18. Habener J. F., Kemp D. M., Thomas M. K. (2005) Minireview: transcriptional regulation in pancreatic development *Endocrinology* 146:1025–1034.
19. Edlund H. (2002) Pancreatic organogenesis—developmental mechanisms and implications for therapy *Nat Rev Genet* 3:524–532.
20. Edlund H. (2001) Developmental biology of the pancreas *Diabetes* 50:55–9.
21. Bort R., Zaret K. (2002) Paths to the pancreas *Nat Genet* 32:85–86.
22. Chakrabarti S. K., Mirmira R. G. (2003) Transcription factors direct the development and function of pancreatic beta cells *Trends Endocrinol Metab* 14:78–84.
23. Hogan K. A., Bautch V. L. (2004) Assembly and Patterning of Vertebrate Blood Vessels *Curr Top Dev Biol* 62:55–85.
24. Lammert E., Cleaver O., Melton D. (2001) Induction of Pancreatic Differentiation by Signals from Blood Vessels *Science* 294:564–567.
25. Nikolova G., Lammert E. (2003) Interdependent development of blood vessels and organs *Cell Tissue Res* 314:33–42.
26. Hebrok M., Kim S. K., Melton D. A. (1998) Notochord repression of endodermal Sonic hedgehog permits pancreas development *Genes Dev* 12:1705–1713.
27. Apelqvist A., Ahlgren U., Edlund H. (1997) Sonic hedgehog directs specialised mesoderm differentiation in the intestine and pancreas *Curr Biol* 7:801–804.
28. Jonsson J., Carlsson L., Edlund T., Edlund H. (1994) Insulin-promoter-factor 1 is required for pancreas development in mice *Nature* 371(6498):606–609.
29. Offield M. F., Jetton T. L., Labosky P. A., Ray M., Stein R. W., Magnuson M. A., Hogan B. L., Wright C. V. (1996) PDX-1 is required for pancreatic outgrowth and differentiation of the rostral duodenum *Development* 122(3):983–995.
30. Ahnfelt-Ronne J., Jorgensen M. C., Hald J., Madsen O. D., Serup P., Hecksher-Sorensen J. (2007) An Improved Method for Three-dimensional Reconstruction of Protein Expression Patterns in Intact Mouse and Chicken Embryos and Organs *J Histochem Cytochem* 55:925–930.
31. Jorgensen M. C., Ahnfelt-Ronne J., Hald J., Madsen O. D., Serup P., Hecksher-Sorensen J. (2007) An Illustrated Review of Early Pancreas Development in the Mouse *Endocr Rev* 28:685–705.
32. Herrera P. L., Nepote V., Delacour A. (2002) Pancreatic Cell Lineage Analyses in Mice *Endocrine* 19:267–278.
33. Ghosh R., Tomlin C. (2004) Symbolic Reachable Set Computation of Piecewise Affine Hybrid Automata and its Application to Biological Modelling: Delta-Notch Protein Signalling *Syst Biol (Stevenage)* 1:170–183.
34. Marnellos G., Deblandre G. A., Mjolsness E., Kintner C. (2000) Delta-Notch Lateral Inhibitory Patterning In The Emergence Of Ciliated Cells In Xenopus: Experimental Observations And A Gene Network Model *Pac Symp Biocomput* pp. 329–340.
35. Matsuno H., Murakami R., Yamane R., Yamasaki N., Fujita S., Yoshimori H., Miyano S. (2003) Boundary formation by notch signaling in Drosophila multicellular systems: experimental observations and gene network modeling by Genomic Object Net *Pac Symp Biocomput* pp. 152–163.
36. Kawahira H., Scheel D. W., Smith S. B., German M. S., Hebrok M. (2005) Hedgehog signaling regulates expansion of pancreatic epithelial cells *Dev Biol* 280:111–121.
37. Kim S. K., Hebrok M., Melton D. A. (1997) Notochord to endoderm signaling is required for pancreas development *Development* 124:4243–4252.
38. Yoshitomi H., Zaret K. S. (2004) Endothelial cell interactions initiate dorsal pancreas development by selectively inducing the transcription factor Ptf1a *Development* 131:807–817.
39. Rossi J. M., Dunn N. R., Hogan B. L., Zaret K. S. (2001) Distinct mesodermal signals, including BMPs from the septum transversum mesenchyme, are required in combination for hepatogenesis from the endoderm *Genes Dev* 15:1998–2009.
40. Dong P. D., Munson C. A., Norton W., Crosnier C., Pan X., Gong Z., Neumann C. J., Stainier D. Y. (2007) Fgf10 regulates hepatopancreatic ductal system patterning and differentiation *Nat Genet* 39:397–402.
41. Miralles F., Lamotte L., Couton D., Joshi R. L. (2006) Interplay between FGF10 and Notch signalling is required for the self-renewal of pancreatic progenitors *Int J Dev Biol* 50:17–26.

42. Bhushan A., Itoh N., Kato S., Thiery J. P., Czernichow P., Bellusci S., Scharfmann R. (2001) Fgf10 is essential for maintaining the proliferative capacity of epithelial progenitor cells during early pancreatic organogenesis *Development* 128:5109–5117.
43. Lammert E., Cleaver O., Melton D. (2003) Role of endothelial cells in early pancreas and liver development *Mech Dev* 120:59–64.
44. Zaret K. S. (2001) Hepatocyte differentiation: from the endoderm and beyond *Curr Opin Genet Dev* 11:568–574.
45. Hogan B. L., Yingling J. M. (1998) Epithelial-Mesenchymal Interactions in Lung Development *Curr Opin Genet Dev* 8:481–486.
46. Hogan B. L. (1999) Morphogenesis *Cell* 96:225–233.
47. Weaver M., Dunn N. R., Hogan B. L. (2000) Bmp4 and Fgf10 play opposing roles during lung bud morphogenesis *Development* 127:2695–2704.
48. Wells J. M., Melton D. A. (1999) Vertebrate endoderm development *Annu Rev Cell Dev Biol* 15:393–410.
49. Axelrod J. D. (2006) Cell Shape in Proliferating Epithelia: A Multifaceted Problem *Cell* 126:643–645.
50. Ciliberto A., Novak B., Tyson J. J. (2003) Mathematical Model of the Morphogenesis Checkpoint in Budding Yeast *J Cell Biol* 163:1243–1254.
51. Gibson M. C., Patel A. B., Nagpal R., Perrimon N. (2006) The emergence of geometric order in proliferating metazoan epithelia *Nature* 442:1038–1041.
52. Nelson C. M., Vanduijn M. M., Inman J. L., Fletcher D. A., Bissell M. J. (2006) Tissue geometry determines sites of mammary branching morphogenesis in organotypic cultures *Science* 314:298–300.
53. Prusinkiewicz P., Rolland-Lagan A. G. (2006) Modeling plant morphogenesis *Curr Opin Plant Biol* 9:83–88.
54. Setty Y., Cohen I. R., Mayo A. E., Harel D. (2008) On Using Divide and Conquer in Modeling Natural Systems, in *Algorithmic Bioprocesses*, to appear.
55. Noble D. (2002) The Heart Cell In Silico: Successes, Failures and Prospects *Novartis Found Symp* 247:182–194; discussion 194–187, 198–206, 244–152.
56. Harel D. (2005) A Turing-like test for biological modeling *Nat Biotechnol* 23:495–496.
57. Cohen I. R. (2007) Modeling immune behavior for experimentalists *Immunol Rev* 216:232–236.
58. Harel D. (2003) A Grand Challenge for Computing: Full Reactive Modeling of a Multi-Cellular Animal *Bulletin of the EATCS* 81:226–235.
59. Cohen I.R. (2000) Tending Adam's Garden: Evolving the Cognitive Immune Self *London: Academic Press*.
60. Harel D., Gery E. (1997) Executable Object Modeling with Statecharts *Computer* 30:31–42, Also in *Proc. 18th Int. Conf. Soft. Eng., Berlin, IEEE Press, March, 1996*, pp. 246–257.
61. Turing A. M. (1990) The chemical basis of morphogenesis. 1953 *Bull Math Biol* 52:153–197; discussion 119–152.
62. Turing A. M. (1952) The Chemical Basis of Morphogenesis *Philos. Trans. R. Soc. London B* 237:37–72.
63. Fleischer K. W., Barr A. H. (1994) A simulation testbed for the study of multicellular development: The multiple mechanisms of morphogenesis., in *Artificial Life III*, Addison-Wesley, pp. 389–416.

Fig. 1. Illustration of early stages of pancreatic organogenesis (embryonic day 9-12; adopted from [19]).

Fig. 2. Modeling an autonomous cell. The three objects, Cell, Nucleus and Membrane, accompanied by some of their Statechart. Note: Unexp. and Exp. states are abbreviations for Unexpressed and Expressed states of the Nucleus object.

Fig. 3. Modeling the extracellular space. Top: An illustration of the participating tissues (adopted from [13]). Middle: The 3D animated front-end of the model. Bottom: The interaction scheme between elements in the model.

Fig. 4. Pancreatic organogenesis: Top: histological images of the pancreas at three different stages (adopted from [19]). Bottom: *in silico* snapshots of the morphogenesis emerging from our model.

Fig. 5. Morphogenesis of the pancreas at 4 different time points: illustration (left; adopted from [13]), a 2D cross section of the simulated structure (middle) and the 3D emerging structure (right)

Fig. 6. Histological cross-section image vs. the simulation at embryonic day 10 (top left image was adopted from [11]). Notice the emerging Pdx1-negative red clusters in the simulation.

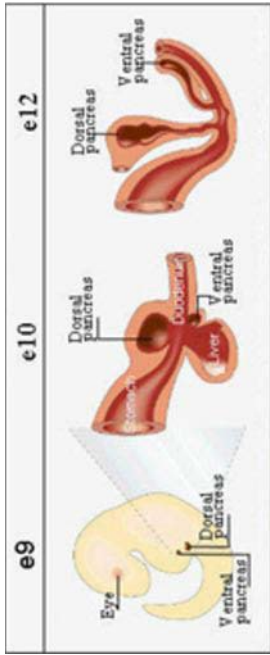
Fig. 7. Left: Analysis of Pdx1-negative cells over time in five runs of the simulation. The maximum is achieved at day 10, with an average of ~4%. Right: Morphogenetic pattern of the Delta-Notch mechanism: endocrine cells (purple) scattered among pancreatic precursor cells (green). The simulation achieved ~15% endocrine cells at equilibrium after one embryonic day (bottom-right graph).

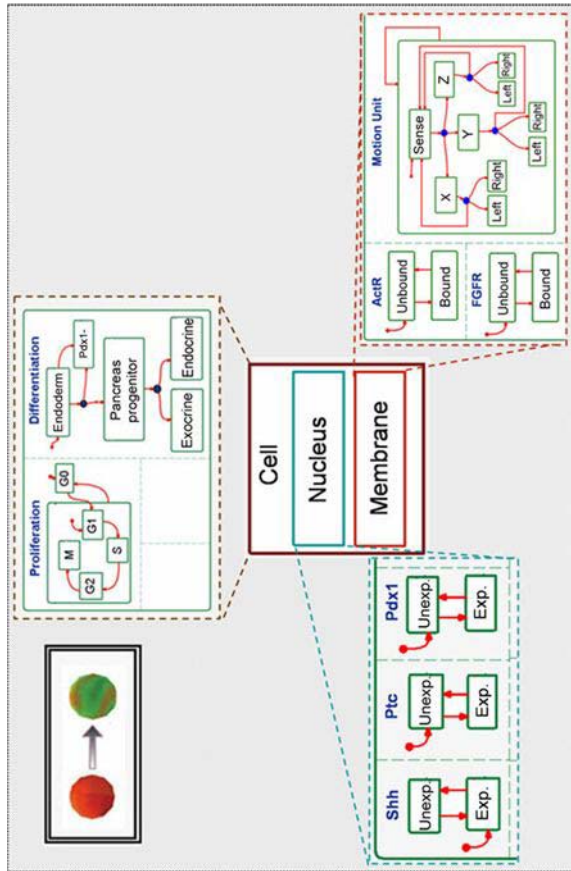
Fig. 8. Validating the emergent property using image processing methods. Left: the domain of pancreatic precursor tissue (Pdx1-positive) in the pancreatic bud. Middle: cross-section image of the pancreatic bud at embryonic day 10 (adopted from [11]). Right: the domain of early endocrine (Pdx1-negative) tissue in the pancreatic bud. The analysis revealed that the Pdx1-negative tissue possesses ~6% of the pancreatic bud.

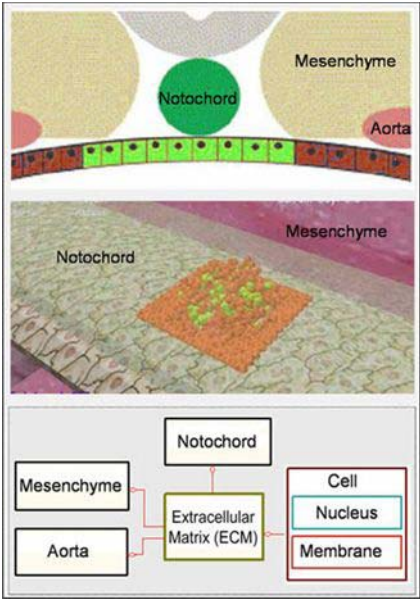
Fig. 9. *In silico* ablation experiments, cell count over time (left) and the emerging 3D structure (middle) and histological images (right; adapted from [19, 37, 38]) (Legend: red and green designate Pdx1-negative and Pdx1-positive cells, black designates total number of cells)

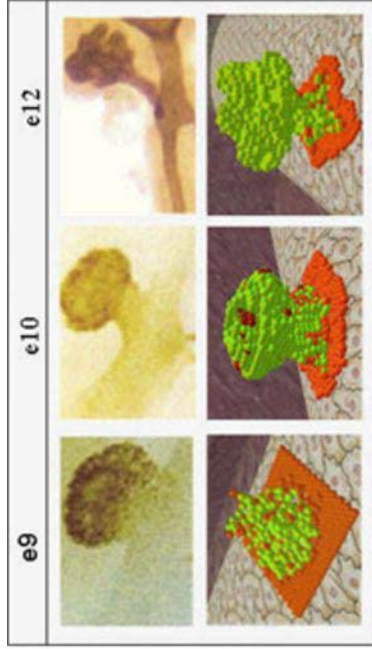
Fig. 10. Pancreatic organogenesis under three levels of expression of BMP4 and FGF10. Branching morphogenesis is promoted by FGF10 (horizontal axis), whereas budding formation is promoted by BMP4 (vertical axis). Notice the hyperplastic morphogenesis and massive apoptosis when both factors are over-expressed.

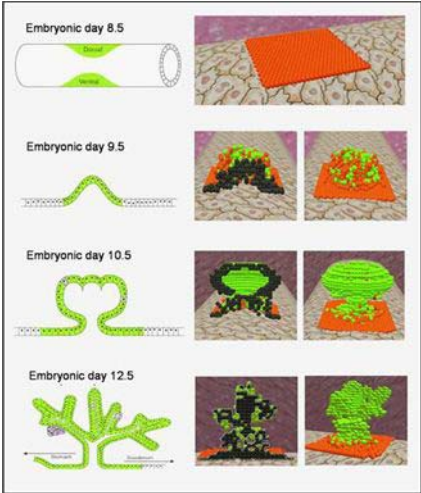
Fig. 11. Different shapes of pancreatic morphogenesis. Left: Lobed formation obtained by a weak uniform expression of FGF10 and strong concentrated expression of BMP4. Right: Branched formation obtained by a scattered expression of FGF10 and a uniform expression of BMP4.

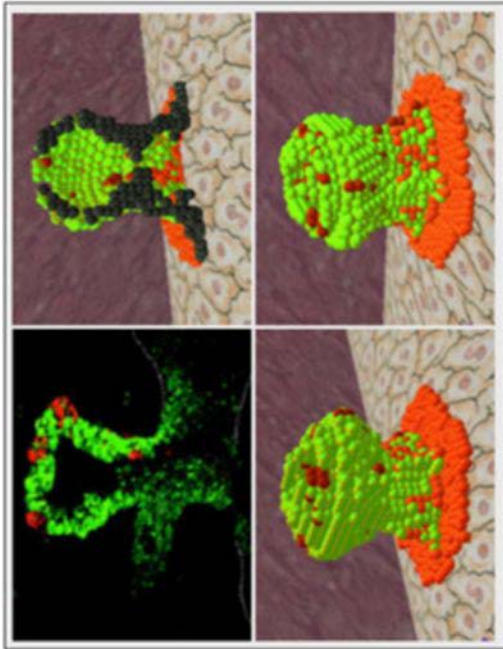


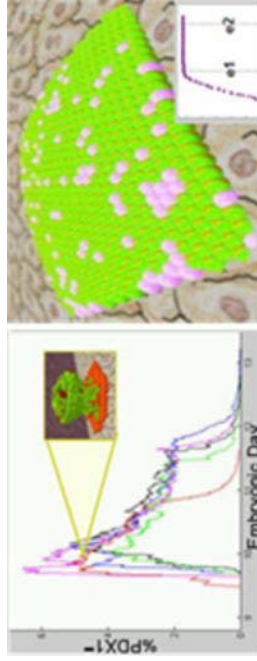


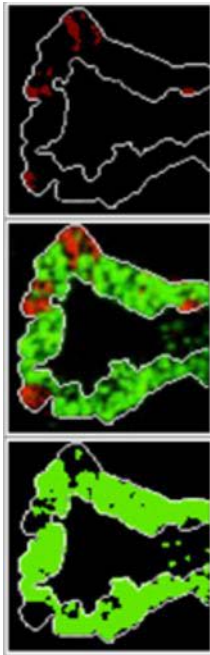


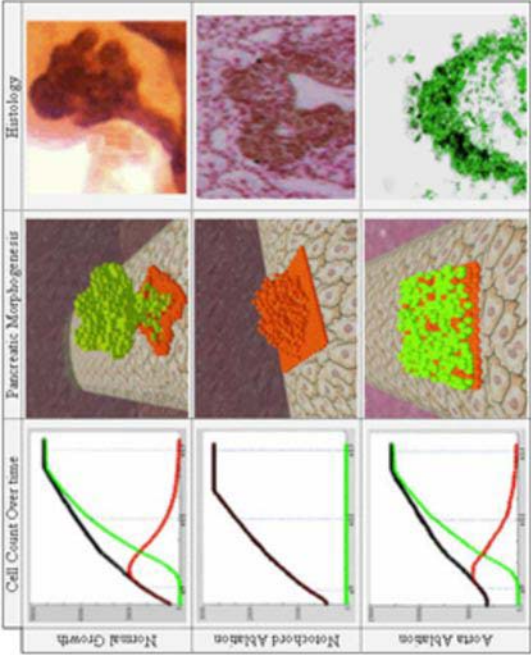


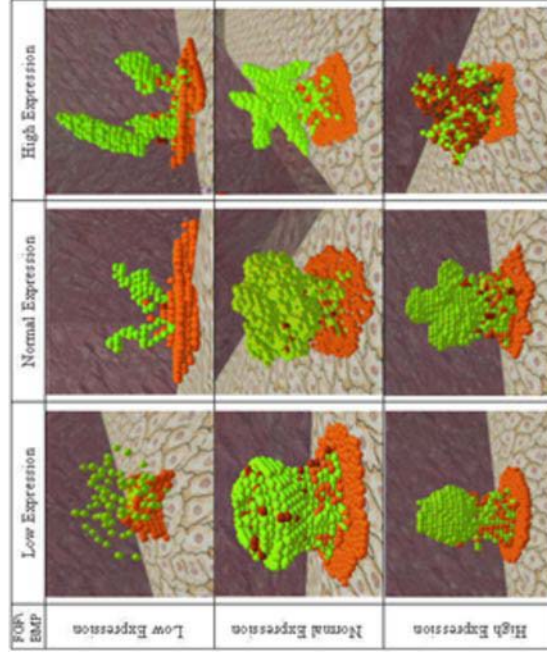


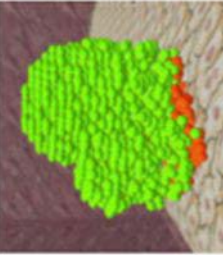
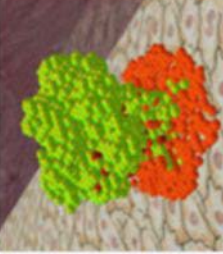
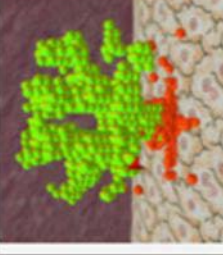










Liver	
Highly lobed pancreas	
Pancreas	
Highly branched pancreas	
Lungs	